Viscosity and phase state of aerosol particles consisting of sucrose mixed with inorganic salts

Young-Chul Song[1,2], Joseph Lilek[3], Jae Bong Lee[4], Man Nin Chan[5,6], Zhijun Wu[7], Andreas Zuend[3], Mijung Song[1,2,8,*]

[1]Department of Earth and Environmental Sciences, Jeonbuk National University, Republic of Korea
[2]The Earth and Environmental Science System Research Center, Jeonbuk National University, Republic of Korea
[3]Department of Atmospheric and Oceanic Sciences, McGill University, Montréal, Quebec, Canada
[4]Inovative System Safety Research Division, Korea Atomic Energy Research Institute, Republic of Korea
[5]Earth System Science Programme, Faculty of Science, The Chinese University of Hong Kong, Hong Kong, China
[6]The Institute of Environment, Energy, and Sustainability, The Chinese University of Hong Kong, Hong Kong, China
[7]Key Joint Laboratory of Environmental Simulation and Pollution Control, College of Environmental Sciences and Engineering, Peking University, Beijing 100871, China
[8]Department of Environment and Energy, Jeonbuk National University, Republic of Korea

Correspondence: Mijung Song (mijung.song@jbnu.ac.kr)

Abstract

Research on the viscosity and phase state of aerosol particles is essential because of their significant influence on the particle growth rate, equilibration times and related evolution of mass concentration as well as heterogeneous reactions. So far, most studies of viscosity and phase state have been focused on organic aerosol particles, yet data on how viscosity can vary when the organic materials are mixed with inorganic salts remain scarce. Herein, using a bead-mobility and a poke-and-flow technique, we

quantified viscosities at 293 ± 1 K for binary mixtures of organic material/H_2O and inorganic salts/H_2O, as well as ternary mixtures of organic material/inorganic salts/H_2O over the atmospheric relative humidity (RH) range. Sucrose as the organic species, and calcium nitrate ($Ca(NO_3)_2$) or magnesium nitrate ($Mg(NO_3)_2$) as the inorganic salts were examined. For binary sucrose/H_2O particles, the viscosities gradually increased from ~3×10^{-2} to > ~1×10^8 Pa s as RH decreased from ~75% to ~25%. Compared with the results for the sucrose/H_2O particles, binary $Ca(NO_3)_2$/H_2O and $Mg(NO_3)_2$/H_2O particles showed drastic enhancements to > ~1×10^8 Pa s at low RH close to the efflorescence RH. For ternary mixtures of sucrose/$Ca(NO_3)_2$/H_2O or sucrose/$Mg(NO_3)_2$/H_2O, with organic-to-inorganic mass ratios of 1:1, the viscosities of the particles gradually increased from ~3×10^{-2} to greater than ~1×10^8 Pa s for RH values from ~75% to ~5%. Compared to the viscosities of the $Ca(NO_3)_2$/H_2O particles, higher viscosities were observed for the ternary sucrose/$Ca(NO_3)_2$/H_2O particles, with values increased by about 1 order of magnitude at 50% RH and about 6 orders of magnitude at 35% RH. Moreover, we applied a thermodynamics-based group-contribution model, AIOMFAC-VISC, to predict aerosol viscosities for the studied systems. The model predictions and viscosity measurements show good agreement within ~ 1 order of magnitude in viscosity. The viscosity measurements indicate that the studied mixed organic–inorganic particles range in phase state from liquid to semi-solid or even solid across the atmospheric RH range at a temperature of 293 K. These results support our understanding that organic/inorganic/H_2O particles can exist in a liquid, semisolid, or even a solid state in the troposphere.

1. Introduction

Aerosol particles are emitted from various natural (e.g., the ocean and plants), and anthropogenic (e.g., transportation and fuel combustion) sources, as well as being produced by gas-to-particle conversion and equilibration processes due to chemical processing of gaseous species in the atmosphere (e.g., sulfur dioxide, nitrogen oxides, ammonia, and volatile organic compounds). Submicron-sized aerosol particles mainly consist of organic materials and inorganic salts (Jimenez et al., 2009; Huang et al., 2015; Cheng et al., 2016). Depending on the location and the season, the organic mass fraction of submicron particles ranges from ~20% up to ~90% (Zhang et al., 2007, 2015a; Jimenez et al., 2009; Hao et al., 2014; Huang et al., 2015; Cheng et al., 2016; Wang et al., 2016). Field measurements have shown that organic materials

and inorganic salts are often internally mixed in an aerosol particle (Murphy et al., 2006; Song et al., 2010, 2013). They can significantly affect the local air quality (Kulmala et al., 2011; Wang et al., 2015a; Zhang et al., 2015a; Schmedding et al., 2020), regional climate (Russell et al., 1997; Kaufman et al., 2002; Kanakidou et al., 2005; Kulmala et al., 2011), and human health (Bhattarai et al., 2019). However, the physicochemical properties of internally mixed particles such as the relative humidity (RH) dependent viscosities and morphologies remain poorly characterized.

The viscosity of aerosols can vary based on the RH and related water uptake, chemical composition, and temperature, with effects on the size distribution (Shiraiwa et al., 2013; Zaveri et al., 2014, 2018), mass concentration of aerosol particles (Shiraiwa and Seinfeld, 2012; Yli-Juuti et al., 2017; Kim et al., 2019), ice nucleation efficiency (Murray et al., 2010; Ladino et al., 2014; Knopf et al., 2018), and crystallinity of salts (Murray, 2008; Song et al., 2013; Ji et al., 2017; Wang et al., 2017). Depending on the viscosity, the phase state of aerosol particles can be determined; commonly the dynamic viscosity of a liquid is characterized as being less than 10^2 Pa s, that of a semi-solid is between 10^2 and 10^{12} Pa s, and that of a glassy or crystalline solid is typically greater than 10^{12} Pa s (Zobrist et al., 2008; Koop et al., 2011; Reid et al., 2018).

Most studies on this topic have focused on the determination of the viscosities and phase state of secondary organic aerosols (SOAs) (Mikhailov et al., 2009; Virtanen et al., 2010; Koop et al., 2011; Vaden et al., 2011; Saukko et al., 2012; Renbaum-Wolff et al., 2013; Hao et al., 2014; Kidd et al., 2014; Bateman et al., 2015; Song et al., 2015, 2016a, 2019; Athanasiadis et al., 2016; Grayson et al., 2016a; Hinks et al., 2016; Hosny et al., 2016; Yli-Juuti et al., 2017; Petters et al., 2019; Wallace and Preston, 2019; Gervasi et al., 2020; Schmedding et al., 2020). Different types of SOAs generated in environmental chambers and flow reactors have been examined. The dynamic viscosities of some types of SOA particles (e.g. generated from toluene and diesel vapors) ranged from $< \sim 10^{-3}$ to $> \sim 10^8$ Pa s, which is approximately equal to the range of viscosities between that of water and tar pitch, depending on the RH, oxidation state, and chemical composition (Mikhailov et al., 2009; Virtanen et al., 2010; Vaden et al., 2011; Koop et al., 2011; Saukko et al., 2012; Renbaum-Wolff et al., 2013a; Hao et al., 2014; Kidd et al., 2014; Bateman et al., 2015; Zhang et al., 2015b; Athanasiadis et al., 2016; Grayson et al., 2016a,b; Hinks et al., 2016; Hosny et al., 2016; Rothfuss and Petters, 2017; Yli-Juuti et al., 2017; Petters et al., 2019; Song et al., 2015,

2016a,b, 2019,2020; Gervasi et al., 2020). In addition to the viscosity of SOA, the viscosity effects of inorganic salts should also be investigated to better understand the viscosities and phase states of atmospherically relevant mixed particles.

Only a few studies have investigated the viscosity and phase state of aerosol particles consisting of organic materials and inorganic salts. Power et al. (2013) showed using holographic optical tweezers that the viscosity of sucrose/H_2O particles is significantly greater than that of NaCl/H_2O particles at any RH. They also showed that the viscosity of mixed sucrose/NaCl/H_2O particles decreased as the NaCl concentration increased at a certain RH. Rovelli et al. (2019) used a different inorganic salt and observed that the viscosity of sucrose/$NaNO_3$/H_2O particles decreased as the $NaNO_3$ mass fraction increased at a certain RH. Richards et al. (2020) reported that inorganic salt in organic and inorganic mixtures increased viscosity by the ion–molecule effect. Based on field measurements using a particle rebound technique, Bateman et al. (2017) showed that the phase state of atmospheric submicron aerosol particles consisting of biogenic organic compounds, sulfate, and black carbon in central Amazonia assumed a nonliquid state (i.e. viscosity > 10^2 Pa s) even at relatively high RH values during periods of anthropogenic influence. They reported that the aerosol particles influenced by a plume of urban pollution and biomass burning existed in a non-liquid state (viscosity > 10^2 Pa s). Liu et al. (2019) observed atmospheric submicron aerosol particles in a liquid phase state at RH > 60% upon the enhancement of the aerosol nitrate fraction in Shenzhen, which is a subtropical coastal urban city in China. Considering the wide variety of complex atmospheric aerosol compositions, more information on the viscosity of mixed organic–inorganic particles is needed.

Using the bead-mobility and poke-and-flow techniques, at 293 ± 1 K, we measured the RH-dependent aerosol viscosities of binary mixtures of organic material/H_2O and inorganic salts/H_2O, and ternary mixtures of organic material/inorganic salts/H_2O under dehydration conditions. Sucrose was selected as the model organic substance because previous studies have frequently applied it as a surrogate species for SOA (Zobrist et al., 2011; Power et al., 2013; Grayson et al., 2016b; Song et al., 2016b; Rothfuss and Petters, 2017; Rovelli et al., 2019). $Ca(NO_3)_2$ and $Mg(NO_3)_2$ were used as model inorganic salts because they have been commonly observed in mineral dust particles (Usher et al., 2003; Laskin et al., 2005; Sullivan et al., 2007), and sea-salts (Gupta et al., 2015; Zieger et al., 2017) in the atmosphere (Usher et

al., 2003; Laskin et al., 2005; Sullivan et al., 2007; Shi et al., 2008; Song et al., 2010, 2013; Pan et al., 2017). Moreover, both of these nitrate salts have a relatively low efflorescence RH in aqueous solutions, enabling viscosity measurements of crystal-free solutions from high RH down to at least 30 % RH. Using these binary and ternary mixtures, we explore how the viscosities vary as a function of RH and associated aerosol compositions. Such viscosity studies can provide a better knowledge of the physicochemical properties of atmospherically relevant aerosol particles consisting of organic material and inorganic salts.

2. Experimental

2.1 Generation of particles

Sucrose (99.5% purity, Sigma-Aldrich), $Ca(NO_3)_2 \cdot 4\,H_2O$ (99.997% purity, Sigma-Aldrich), and $Mg(NO_3)_2 \cdot 6H_2O$ (99.99% purity, Sigma-Aldrich) were purchased. Solutions containing each compound were prepared at 10 wt. % in pure water (resistivity ≥ 18.2 MΩ cm, Merck Millipore Synergy, Germany). For ternary mixtures, solutions were prepared at an organic-to-inorganic dry mass ratio (OIR) of 1:1. This dry mass ratio was chosen since it is expected to reveal well the effects of mixing of substantial amounts of both the organic and salt components on overall water uptake and viscosity. For the bead-mobility and poke-and-flow experiments, the aqueous solutions were nebulized on a hydrophobic substrate (Hampton Research, Canada). After nebulizing, the substrate with droplets was set in a flow-cell which was placed below an objective mounted on an optical microscope (Olympus CKX53 with 40× objective) (Pant et al., 2006; Bertram et al., 2011; Song et al., 2012; Ham et al., 2019). The RH in the cell was adjusted by controlling the N_2 mixing ratio of the dry and wet gas flows. The RH in the flow-cell was continuously monitored by a digital humidity sensor (Sensirion, SHT C3, Switzerland). The RH reading from the flow-cell was calibrated by measurement and comparison to the deliquescence RH (DRH) at 293 ± 1 K of saturated aqueous solutions of ammonium sulfate (80.5%), sodium chloride (76.0%), and potassium carbonate (44.0%) (Winston and Bates, 1960). The uncertainty of the RH of the humidified N_2 flow was ± 1.5% RH based on the calibration tests. At the initiation of the bead-mobility and poke-and-flow experiments, the RH was maintained at ~85% and the particles equilibrated for ~20 min. Then, the RH was reduced to the target RH (~80 – ~0% RH) and equilibrated for ~30 min for the bead-mobility experiments, and for > ~2 hours for the poke-and-flow experiments to give sufficient time for reaching

equilibrium with the surrounding water vapour (Grayson et al., 2015, Song et al., 2019; Maclean et al., 2021). At a given RH, particles that were 20 – 100 μm in diameter were selected for the optical observation. All viscosity measurements were carried out at a temperature of 293 ± 1 K.

2.2 Bead-mobility technique

The bead-mobility technique was utilized, which can quantify a range of viscosities from ~10^{-3} to ~10^{3} Pa s (Renbaum-Wolff et al., 2013b). At the beginning of the bead-mobility experiments, insoluble melamine beads (Cat. no. 86296, Sigma-Aldrich), which were ~1 μm in diameter and dispersed in pure water, were incorporated directly into the droplets deposited on the hydrophobic substrate. Aerosol particles were then placed into the flow-cell, as described in Sect. 2.1. The total gas flow in the cell was 1200 sccm for the bead-mobility experiments. The continuous gas flow generates a shear stress on a particle's surface, which yields internal circulations of the beads in the particles during measurements. The movement of the beads at 293 ± 1 K was recorded every 1 s with a CMOS camera (MSC-M 3.0 UCMOS, China) and then quantified at a target RH. The viscosity was calculated from the bead speeds using a calibration line, which produced bead speeds for the sucrose particles at different RH values (see Fig. S1 of the Supplement). Figure S2 illustrates the mean bead speeds of each system as a function of the RH. When the bead speeds within a particle are too slow to be observed with this technique (i.e. below ~10^{-6} μm · m s^{-1} corresponding to ~10^{2} Pa s, see Fig. S1 and S2), we used the poke-and-flow technique (Sect. 2.3). For example, the movement of the beads within $Mg(NO_3)_2/H_2O$ particles at ~35% RH was too slow to be readily observed (Fig. S2). Further information on the calibration and the bead-mobility technique is given in Sect. S1 in the Supplement.

2.3 Poke-and-flow technique

Murray et al. (2012) developed the poke-and-flow technique for phase state determination, which was expanded for the quantification of viscosities > ~10^{2} Pa s by Renbaum-Wolff et al. (2013a), Grayson et al. (2015), and Song et al. (2015). This technique uses a small hole on the top of the flow-cell to allow us to poke the particles on the hydrophobic substrate using a sterilized sharp needle (Jung Rim Medical Industrial Co., South Korea). Using a micromanipulator (Narishige, model MO-152, Japan), the needle

was controlled in the *x*-, *y*-, *z*-direction. The needle was passed through from the top to the bottom of a particle and then the needle was removed. After poking, the geometrical change of a deposited particle was observed and recorded by an optical microscope (Olympus CKX53 with 40× objective) with a CCD camera (MSC-M 3.0 UCMOS, China). All experiments were carried out at 293 ± 1 K.

Figure S3 shows an example of the geometrical changes in the sucrose/H_2O, sucrose/$Ca(NO_3)_2/H_2O$, and sucrose/$Mg(NO_3)_2/H_2O$ particles during pre-poking, poking, and post-poking. Before poking by the needle, the particles had a geometry of a spherical cap. After poking by a needle, a half-torus geometry with an inner hole in the particle was observed. As time progressed, the particle recovered by adopting its original geometry by filling of the hole to minimize the surface energy. The experimental flow time ($\tau_{(exp,\ flow)}$) was obtained when the area of the inner hole just after poking (t = 0 s. Fig. S3) decreased to 1/4 of the initial inner hole area (Renbaum-Wolff et al., 2013a; Grayson et al., 2015, 2016; Song et al., 2019). Figure S4 shows the $\tau_{(exp,\ flow)}$ at different RH for sucrose/H_2O, sucrose/$Mg(NO_3)_2/H_2O$, and sucrose/$Ca(NO_3)_2/H_2O$ particles. The $\tau_{(exp,\ flow)}$ of the particles was converted to the lower limit to the viscosity using the equation reported in Sellier et al. (2015). Using the poke-and-flow technique, the upper limit to viscosity is unknown in this work. For binary mixtures of inorganic salts/H_2O, we were unable to determine the viscosity between 10^2 to 10^8 Pa s because the poke-and-flow technique is not accessible for droplets that are supersaturated with respect to a crystalline state of involved inorganic salts. We also measured the RH value and corresponding viscosity at which the particles cracked. When the particles cracked upon poking, without any detectable flow after a duration of > 5 h at a given RH, we defined a lower limit to the viscosity of 1×10^8 Pa s based on the results of Renbaum-Wolff et al. (2013a), Grayson et al. (2015, 2016), and Song et al. (2019). Further details on these experiments can be found in Sect. S2 of the Supplement.

2.4 AIOMFAC-VISC model

The Aerosol Inorganic–Organic Mixtures Functional groups Activity Coefficients Viscosity model (AIOMFAC-VISC) is a thermodynamics-based group-contribution model for predicting the viscosity of aqueous organic mixtures (Gervasi et al., 2020). It is an extension module to the AIOMFAC model, which explicitly describes interactions among organic functional groups, inorganic ions, and water (Zuend et al.,

2008, 2011). The AIOMFAC-VISC model offers predictive estimates of mixture viscosity covering the range from liquid-like, low-viscosity aqueous solutions to highly viscous, organic-rich amorphous solutions in the atmospherically relevant temperature range. An online version of AIOMFAC (AIOMFAC-web), which includes viscosity predictions for aqueous organic mixtures, can be run at https://aiomfac.lab.mcgill.ca.

Aside from the focus on the viscosity effects of organic compounds, in recent work AIOMFAC-VISC has been further developed to enable the prediction of the viscosity of aqueous electrolyte solutions and aqueous inorganic–organic mixtures; with details provided elsewhere (Lilek et al., *in preparation*). Briefly, a semi-empirical approach was introduced to predict the mixture viscosity of aqueous electrolyte solutions as a function of temperature, ion activities, and ionic strength. Model parameters for the aqueous ion interaction approach were simultaneously fitted to room temperature viscosity measurements aggregated by Laliberté for many electrolyte solutions (Laliberté, 2007, 2009). The training dataset for AIOMFAC-VISC did not include measurements for the nitrate salts investigated in this study. For aqueous electrolyte solutions, AIOMFAC-VISC predictions currently achieve an excellent level of accuracy, comparable to that of the fitted expressions by Laliberté (2007). Furthermore, to more accurately capture the water uptake behavior of sucrose as a function of equilibrium RH (i.e. water activity of the solution), the version of AIOMFAC-VISC used to produce the viscosity predictions for the sucrose-containing systems in this work includes an improved treatment of the ether-group–water interactions of sucrose. Thus, viscosity predictions in this study for aqueous sucrose differ slightly from those of the AIOMFAC-web model version.

For the viscosities of ternary mixtures, a Zdanovskii-Stokes-Robinson (ZSR) type mixing rule is applied to predict the viscosity of the ternary mixtures of organic material/inorganic salts/H_2O. This mixing rule is here adopted for viscosity applications since the AIOMFAC-VISC model does presently not include explicit ion–organic interaction effects on viscosity (only on activity coefficients). Therefore, a mixing rule is required to combine the predictions of the viscosity contributions from the electrolyte-free subsystem (sucrose/H_2O) and those from the organic-free aqueous electrolyte subsystem for the viscosity estimation of the full mixture. Generally, the ZSR approach involves combining some physical property of two or more (binary) mixtures at the same RH, often to determine the water content of the whole

multicomponent mixture (Zdanovskii, 1936, 1948; Stokes and Robinson, 1966). Following the experimental conditions, the AIOMFAC-VISC predictions for the ternary systems use an OIR of 1:1, which constrains at each RH level the fractional contributions of mass (f_1, f_2) from each of the subsystems, sucrose/H_2O (1) or salt/H_2O (2). The viscosity of the overall mixture is then obtained as $\ln(\eta/\eta^\circ) = f_1 \ln(\eta_1/\eta^\circ) + f_2 \ln(\eta_2/\eta^\circ)$, with η° denoting unit viscosity (1 Pa s); see details in section S5 of the Supplement.

3. Results and discussion

3.1 Viscosities of particles consisting of sucrose/H_2O

Figure 1 shows the RH-dependent viscosities of sucrose/H_2O particles obtained using the bead-mobility and poke-and-flow techniques. The viscosities of sucrose/H_2O particles were determined to be between ~2×10^{-1} and ~1×10^{1} Pa s for RH values of ~85– 69%, and between ~5×10^{3} and ~2×10^{6} Pa s for RH values of ~50 – 37% (Fig. 1). The particles containing sucrose/H_2O cracked at ~23% RH when poked with a needle, and restorative flow did not occur over a time span of 5 h (Fig. 2a). Consequently, only a lower limit for the viscosity of ~10^{8} Pa s was obtained (Renbaum-Wolff et al., 2013a; Grayson et al., 2015, 2016; Song et al., 2015a, 2019). Figure 1 also includes results from previous studies for the viscosities of sucrose/H_2O particles using different techniques such as bead-mobility, poke-and-flow, holographic optical tweezers, and fluorescence lifetime imaging microscopy (Hosny et al., 2013, Power et al. 2013, Grayson et al., 2015, Song et al., 2015, 2016b). As shown in Fig. 1, the viscosities for the sucrose/H_2O particles from this study and previous studies are consistent within ~ 1 order of magnitude at given RH values. Using the entire dataset, it suggests that the sucrose/H_2O particle are in a liquid phase state for RH > ~65%, in a semi-solid phase state for ~25% < RH < ~65%, and in a semi-solid or solid phase state for RH < ~23%.

3.2 Viscosities of particles consisting of $Mg(NO_3)_2/H_2O$ or $Ca(NO_3)_2/H_2O$

Despite the abundant mass of inorganic species in the atmosphere (Jimenez et al., 2009; Cheng et al., 2016), few studies have reported the viscosity of single particles consisting of inorganic species covering the RH range to high salt concentrations (Power et al., 2013; Rovelli et al., 2019). Herein, the RH-

dependent viscosity was quantified for particles consisting of $Mg(NO_3)_2/H_2O$ or $Ca(NO_3)_2/H_2O$ determined at 293 ± 1 K upon dehydration using the bead-mobility and poke-and-flow techniques.

Figure 3 illustrates the RH-dependent viscosities of $Mg(NO_3)_2/H_2O$ or $Ca(NO_3)_2/H_2O$ particles upon dehydration. The obtained viscosities of the $Mg(NO_3)_2/H_2O$ particles varied from ~6×10^{-3} to ~4×10^{-2} Pa s for RH values from ~70 to ~35% whereas the values for $Ca(NO_3)_2/H_2O$ ranged from ~3×10^{-2} to ~9×10^{1} Pa s for RH values from ~65 to ~10%. Previous studies have reported the viscosities of $Ca(NO_3)_2/H_2O$ and $Mg(NO_3)_2/H_2O$ solutions only at high RH values based on bulk solution measurements (Fig. 3) (Abdulagatov et al., 2004; Wahab et al., 2006). The values of the viscosities of the particles at high RH are consistent with our results within ~ 1 order magnitude despite a limited number of data points due to the solubility limit restricting bulk solution measurements to the RH range above 70 %. In addition, Fig. 3 shows the viscosities of $NaNO_3/H_2O$ particles measured by other groups (Haynes, 2015; Rovelli et al., 2019). The viscosities of the $NaNO_3/H_2O$ particles were similar to those of the $Ca(NO_3)_2/H_2O$ particles for the RH range from ~30 to ~100 %.

During the poke-and-flow experiments, the $Mg(NO_3)_2/H_2O$ or $Ca(NO_3)_2/H_2O$ particles cracked when poked with a needle at RH values of 30% and 5%, respectively. At these RH levels, noticeable restorative flow did not occur for over 5 h (Fig. 2b and c), which resulted in a lower estimated limit for the viscosity (~10^8 Pa s) at the given RH values. The RH value where the particles shattered is similar to the efflorescence RH (ERH) of $Mg(NO_3)_2/H_2O$. The ERH of $Mg(NO_3)_2/H_2O$ is known to be ~30% at 298 K (Li et al., 2008; Wang et al., 2015b) and RH of crystallization for $Ca(NO_3)_2/H_2O$ is reported to be ~7% at 298 K (Liu et al., 2008). In this study, we optically observed an ERH of 32.0 ± 2.5% for $Mg(NO_3)_2/H_2O$ particles (i.e. Fig. S5b), but we did not optically observe the ERH of $Ca(NO_3)_2/H_2O$ at 293 ± 1 K with decreasing RH (Fig. S5c). Liu et al. (2008) also observed optically no efflorescence point for $Ca(NO_3)_2/H_2O$ particles down to 0% RH using an optical microscope, but they confirmed the crystallization for $Ca(NO_3)_2/H_2O$ particles at RH of ~7% by Raman spectroscopy at 298 K. The RH values at which shattering of particles occurred for the binary inorganic salt particles of $Mg(NO_3)_2/H_2O$ or $Ca(NO_3)_2/H_2O$ were close to their reported ERH values and/or the RH of crystallization. When comparing the two inorganic salts, $Ca(NO_3)_2/H_2O$ particles showed slightly higher viscosities than the $Mg(NO_3)_2/H_2O$ particles, i.e. approximately 1 order of magnitude higher at equivalent RH for the RH

range from ~60 to 30% (Fig. 3). The difference in viscosities is likely due to the higher hygroscopicity of dissolved $Mg(NO_3)_2$ compared to $Ca(NO_3)_2$ (Guo et al., 2019). The $Ca(NO_3)_2/H_2O$ particles were of a liquid phase state at RH > ~10%, and a semi-solid or solid phase state at RH < ~5%. The $Mg(NO_3)_2/H_2O$ particles were of a liquid phase state at RH > ~35%, and a semi-solid or solid phases state at RH < ~30%. Based on the viscosity measurement, both inorganic particles underwent a phase change from liquid ($<10^2$ Pa s) to semi-solid or solid ($>10^2$ Pa s) within a narrow RH range (Fig. 3) compared to the sucrose/H_2O particles (Fig. 1). Indeed, this discontinuity in viscosity with decreasing RH suggests a phase transition.

3.3 Viscosities of particles consisting of sucrose/$Ca(NO_3)_2/H_2O$ or sucrose/$Mg(NO_3)_2/H_2O$

To explore the viscosity of more atmospherically relevant aerosol particle configurations, we investigated ternary systems containing sucrose mixed with either $Ca(NO_3)_2$ or $Mg(NO_3)_2$ for OIR of 1:1 at 293 ± 1 K. Shown in Fig. 4 are the viscosities for the sucrose/$Ca(NO_3)_2/H_2O$ (Fig. 4a) and sucrose/$Mg(NO_3)_2/H_2O$ particles (Fig. 4c) upon dehydration using the bead-mobility and the poke-and-flow measurement techniques.

The viscosities of the sucrose/$Ca(NO_3)_2/H_2O$ particles ranged from ~3×10^1 to ~3×10^{-2} Pa s at ~45 < RH < ~80%, and from ~9×10^5 to ~3×10^4 Pa s at ~25 < RH < ~30% (Fig. 4a). At ~13% RH, when poked with a needle, the sucrose/$Ca(NO_3)_2/H_2O$ particles cracked. Thereafter, the particles did not exhibit any notable flow behavior for over 5 h (Fig. 5a), producing a lower limit for the viscosity of ~10^8 Pa s. This result indicates that the sucrose/$Ca(NO_3)_2/H_2O$ particles were in a liquid phase state at RH > ~ 45%, in a semi-solid state at ~25% < RH < ~30%, and in a semi-solid or solid state for RH < ~13%.

For sucrose/$Mg(NO_3)_2/H_2O$ particles, the viscosities ranged from ~7×10^{-2} to ~1×10^1 Pa s for RH values ranging from ~70 to ~35%, and from ~2×10^4 to ~2×10^5 Pa s for the RH ranging from ~17 to ~11% (Fig. 4c). The sucrose/$Ca(NO_3)_2/H_2O$ particles cracked at ~6% RH without flow over 5 h (Fig. 5b); and thus the lower limit of the viscosity was determined to be ~10^8 Pa s. These results imply that the sucrose/$Ca(NO_3)_2/H_2O$ particles are in a liquid phase state at RH > ~ 35%, a semi-solid phase state for 17% < RH < 11%, and a semi-solid or solid phase state at RH < ~6%. As shown in Figs. 4a and 4c, the viscosities of the sucrose/$Mg(NO_3)_2/H_2O$ particles are approximately 1 order of magnitude lower at 50% RH, and ~6 orders of magnitude lower at 35% RH than the sucrose/$Ca(NO_3)_2/H_2O$ particles over the same

RH range. Both particles experienced a phase state change from a liquid phase state to a semi-solid or even solid phase state with decreasing RH. Finally, although not confirmed by our measurements, it is possible that in one or both of these ternary mixtures a gel phase transition may occur upon sufficient dehydration, as has been observed in mixtures of gluconic acid with $CaCl_2$ (Richards et al., 2020a,b).

3.4 Model–measurement comparison of viscosity

Figure 4b and 4d shows the model–measurement comparison of the RH-dependent viscosities of the binary and ternary systems. For the viscosities of sucrose/H_2O, the viscosities from the AIOMFAC-VISC model prediction agreed with the measurements within ~ 1 order of magnitude. For the viscosities of $Ca(NO_3)_2/H_2O$ and $Mg(NO_3)_2/H_2O$, the viscosity prediction from the AIOMFAC-VISC model showed a good agreement until the measured inorganic salt viscosities change steeply, indicating crystallization or another phase transition that the model ignores. When comparing AIOMFAC-VISC viscosity predictions to the measurements in this study, note that AIOMFAC-VISC assumes that mixtures remain in a metastable state to low water activity (or high solution concentration) and that solutes do not crystallize, which may explain the discrepancy among the model predictions and the measurements in the low RH region shown in Fig. 4b and 4d. Moreover, we note that the training of the AIOMFAC-VISC electrolyte solution model parameters did not include data from this study. The model predictions at RH levels below ~20% represent extrapolations of the model beyond the range of experimental data used in its training.

In AIOMFAC-VISC, the prediction of the temperature-dependent pure-component viscosity is based on the experimentally determined, yet uncertain glass transition RH. As such, we include error thresholds of ± 5% in the pure-component glass transition RH in Fig. 4 (Gervasi et al., 2020). Such uncertainty estimates are not necessary for aqueous electrolyte mixtures, so the AIOMFAC-VISC model sensitivity is shown instead, which is defined as the viscosity change due to a ± 2% change in the mass fraction of water of the solution, while the ratio of the other components is preserved (Gervasi et al., 2020). The uncertainty in the aqueous sucrose viscosity dominates the modelled uncertainty of viscosity estimates for the ternary mixtures. For the viscosities of ternary sucrose/$Ca(NO_3)_2/H_2O$ or sucrose/$Mg(NO_3)_2/H_2O$ solutions, AIOMFAC-VISC viscosity predictions show agreement with the measurements within about 1 order of magnitude from high RH to about 30 % RH (considering measurement uncertainty). In the case

of the ternary sucrose/$Ca(NO_3)_2/H_2O$ system, the model–measurement deviation increases to about 1.5 orders of magnitude in viscosity at 30% RH and lower, with AIOMFAC-VISC underestimating the measured viscosity. This result may be explained at least in part by the model predicting substantially lower viscosities for the binary aqueous $Ca(NO_3)_2$ system in this lower RH range, which affects the predictions for the ternary system via the deployed mixing rule. The good agreement between model and measurements for the ternary sucrose/$Mg(NO_3)_2/H_2O$ system, even at low RH levels, may be interpreted as indicative of suppressed salt crystallization in the presence of sucrose, since no discontinuities in viscosity are observed (in contrast to the measurements for the binary salt particles).

4. Conclusion and atmospheric implications

Herein, we measured the RH-dependent viscosities at 293 ± 1 K for particles consisting of organic material/H_2O, inorganic salt/H_2O, and organic material/inorganic salt/H_2O upon dehydration using the bead-mobility and poke-and-flow techniques. We selected sucrose as the organic species because previous studies have frequently applied it as a surrogate species of SOA and this organic offers favorable properties for measurements. $Ca(NO_3)_2$ and $Mg(NO_3)_2$ were selected as the inorganic salts for viscosity measurements because these inorganic salts have been frequently observed from mineral dust and sea salt particles (Usher et al., 2003; Laskin et al., 2005; Sullivan et al., 2007). For the binary mixtures, the obtained viscosity of the sucrose/H_2O particles agreed well with those reported in previous studies, i.e. mixture viscosities $<10^2$ Pa s at RH > ~65%, which corresponds to a liquid phase state; mixture viscosities of ~10^2 to 10^8 Pa s at RH values between ~65 and ~25%, which correspond to a semi-solid phase state; and mixture viscosities > ~10^8 Pa s at RH < ~25%, which correspond to semi-solid or amorphous (or crystalline) solid phase states (Power et al., 2013; Grayson et al., 2016b; Song et al., 2016b; Rothfuss and Petters, 2017; Rovelli et al., 2019). Upon dehydration, we also quantified the viscosities of the inorganic salts. The viscosities of the $Mg(NO_3)_2/H_2O$ particles were < ~4×10^{-2} Pa s for RH > ~35%, and > ~10^8 Pa s for RH < ~31%, whereas those of the $Ca(NO_3)_2/H_2O$ particles were < ~9×10^0 Pa s for RH > ~10% and > ~10^8 Pa s for RH < ~10%. The particles containing either of these two inorganic salts cracked upon poking when the RH reached a value near the salt's ERH and/or the phase transition RH from a droplet to a solid phase state. These inorganic particles exhibited a sudden enhancement in the viscosity when the

particle effloresced. In contrast, sucrose/H_2O particles showed a smooth enhancement in the viscosity with decreasing RH; this means that the viscosity of sucrose/H_2O particles gradually approached their glass transition RH. The AIOMFAC-VISC model prediction and viscosity measurements showed a good agreement within ~ 1 order of magnitude, especially at RH levels above 30%, where applicable. For sucrose/$Ca(NO_3)_2/H_2O$ particles and sucrose/$Mg(NO_3)_2/H_2O$, predicted and measured viscosities showed good agreement over the whole RH range.

The phase states of aerosol particles have an impact on rate and potential for heterogeneous reactions as well as consequences for the resulting mass concentration of aerosol particles. The uptake coefficient of gas phase oxidants depends on the phase states of aerosol particles (George et al., 2010; Xiao et al., 2011; Kuwata et al., 2012; Slade and Knopf, 2014; Davies and Wilson, 2015; Berkemeier et al., 2016; Li et al., 2020; Xu et al., 2020). For example, ozone uptake coefficients (γO_3) decreased by an order of magnitude in a semi-solid phase state compared to a liquid phase state (Steimer et al., 2015). Moreover, the effective mass concentration of aerosol particles can depend on the (assumed or modelled) phase state of aerosol particles (Shiraiwa and Seinfeld, 2012; Yli-Juuti et al., 2017; Kim et al., 2019). If a liquid aerosol phase state is assumed, the mass concentration may be overpredicted by up to one order of magnitude (Shiraiwa and Seinfeld, 2012). Based on the measurements and calculations, our results show that the studied aerosol particles consisting of organic material/inorganic salt/H_2O range from liquid to semi-solid or solid phase states depending on the RH. A caveat is that a single OIR of 1:1 and relatively simple aerosol systems were used compared to the multicomponent-multiphase particles likely occurring in the real atmosphere (Murphy et al., 2006; Jimenez et al., 2009; Song et al., 2010, 2013; Huang et al., 2015; Cheng et al., 2016). Further studies are needed to confirm the equilibrating timescales of mixed organic–inorganic particles under ambient conditions, including the timescale for the equilibration of semivolatile organics and inorganics. Added complexity in particle morphology, such as phase separation, can also influence the equilibration timescale (e.g. Huang et al. 2021); however, our systems did not exhibit phase separation for the studied mixing ratios. Additional investigations are required to further explore and quantify how the viscosities and phase states of mixed organic–inorganic particles vary with the OIR, temperature, and functional group complexity.

Data availability. Underlying material and related data for this paper are provided in the Supplement.

Author contributions. MS and YS designed this study. MS and JBL setup and calibrated the viscosity instrument. YS and MS conducted viscosity experiments and analyzed the data. JL and AZ conducted AIOMFAC-VISC model predictions. YS and MS prepared the manuscript with contributions from JL, JBL, AZ, ZJ, and MN.

Competing interests. The authors declare that they have no conflict of interest.

Acknowledgements. This work was supported by the National Research Foundation of Korea (NRF) grant funded by the Korea government (MSIT) (NRF-2019R1A2C1086187), and by the Fine Particle Research Initiative in East Asia Considering National Differences (FRIEND) Project (2020M3G1A1114548). This project was undertaken with the financial support of the government of Canada through the federal Department of Environment and Climate Change (grant no. GCXE20S049). This work was also supported by Alfred P. Sloan Foundation under Prime Award no. G-2020-13912 and the Regents of the University of California. M. Song gives thanks to D. Ham for the technical support.

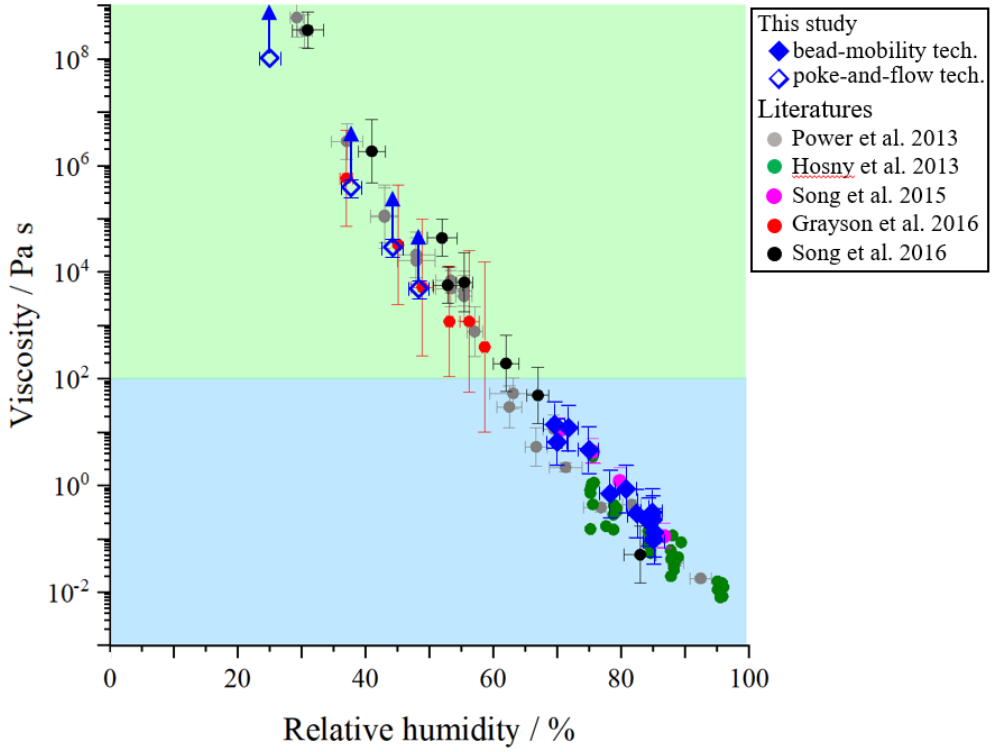

Figure 1. Measured dynamic viscosities of sucrose/H_2O particles compared with previous studies at 293 K (Hosny et al., 2013 (Fluorescent lifetime imaging), Power et al. 2013 and Song et al.2016b (Aerosol optical tweezers), Grayson et al., 2015, Song et al., 2015 (Bead-mobility and Poke-and-flow tech.)) and this study. The error bars in relative humidity (RH) were generated from the calibrated RH uncertainty and the standard deviation from grouped viscosity data (grouped by RH ranges) which included at least 3 data points. The error bars in viscosities were produced by 95% prediction bands of viscosities (Fig. S1). Upward arrows represent lower limit to the viscosities of the particles that calculated by the experimental flow time and the equation reported in Sellier et al. (2015). Details are described in Fig. S2. Light blue and green regions indicate liquid and semi-solid regions, respectively.

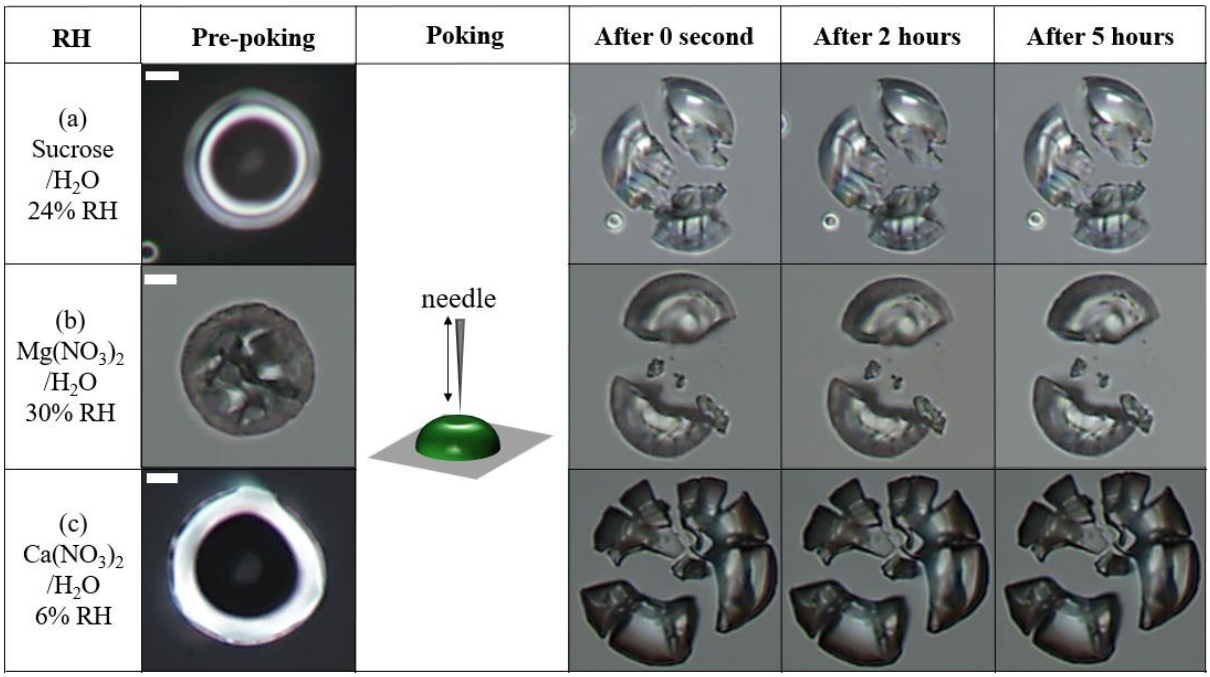

420 Figure 2. Optical images during poke-and-flow experiments at the points of pre-poking, poking, and post-poking for particles consisting of (a) sucrose/H_2O, (b) $Mg(NO_3)_2/H_2O$, and (c) $Ca(NO_3)_2/H_2O$ for relative humidity (RH) where the particles shattered. The scale bar is 5 µm.

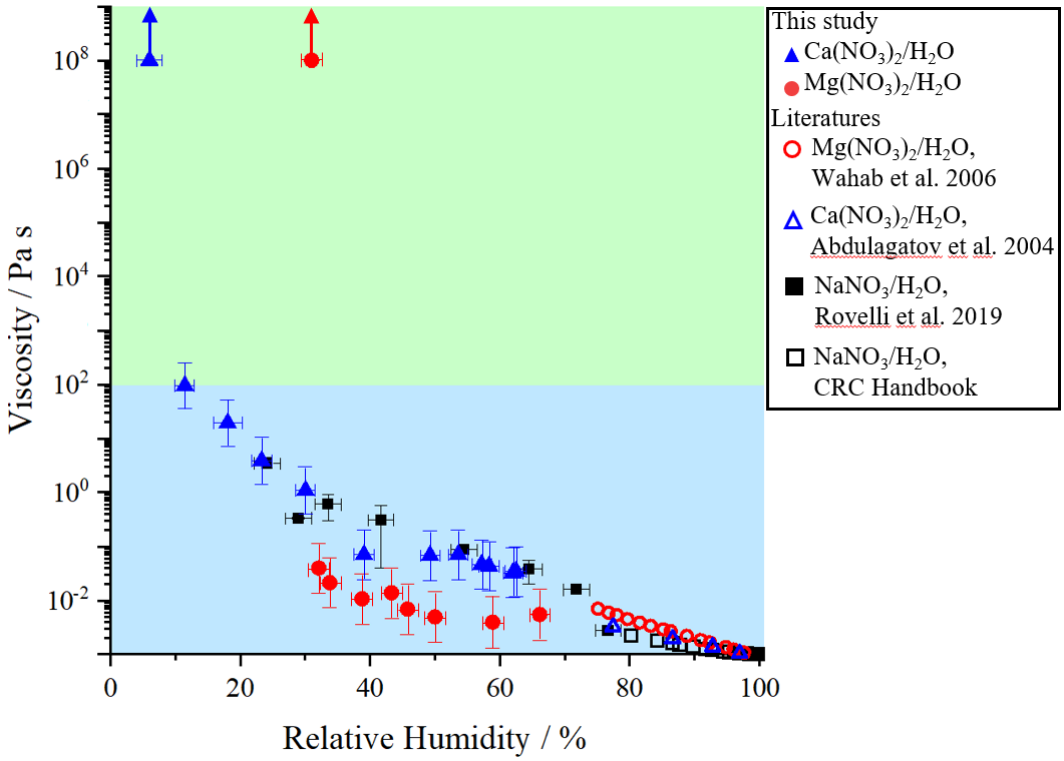

Figure 3. Viscosities of inorganic salts containing $Ca(NO_3)_2/H_2O$ and $Mg(NO_3)_2/H_2O$, and previous results (Abdulagatov et al., 2004; Wahab et al., 2006; Haynes, 2015; bulk measurements) and this study. Also, viscosities of $NaNO_3/H_2O$ from previous studies are included (CRC Handbook; Rovelli et al., 2019 (aerosol optical tweezers)). Upward arrows represent a lower limit for the viscosities of the particles calculated by the experimental flow time and the equation reported in Sellier et al. (2015). The error bars in relative humidity (RH) were generated from combined RH sensor uncertainty and the standard deviation from the grouped viscosity data by RH, which included at least 3 data points. The error bars in viscosities were produced by 95% prediction bands of viscosities (Fig. S1). Light blue region indicates a liquid phase, and light green region indicates a semi-solid phase.

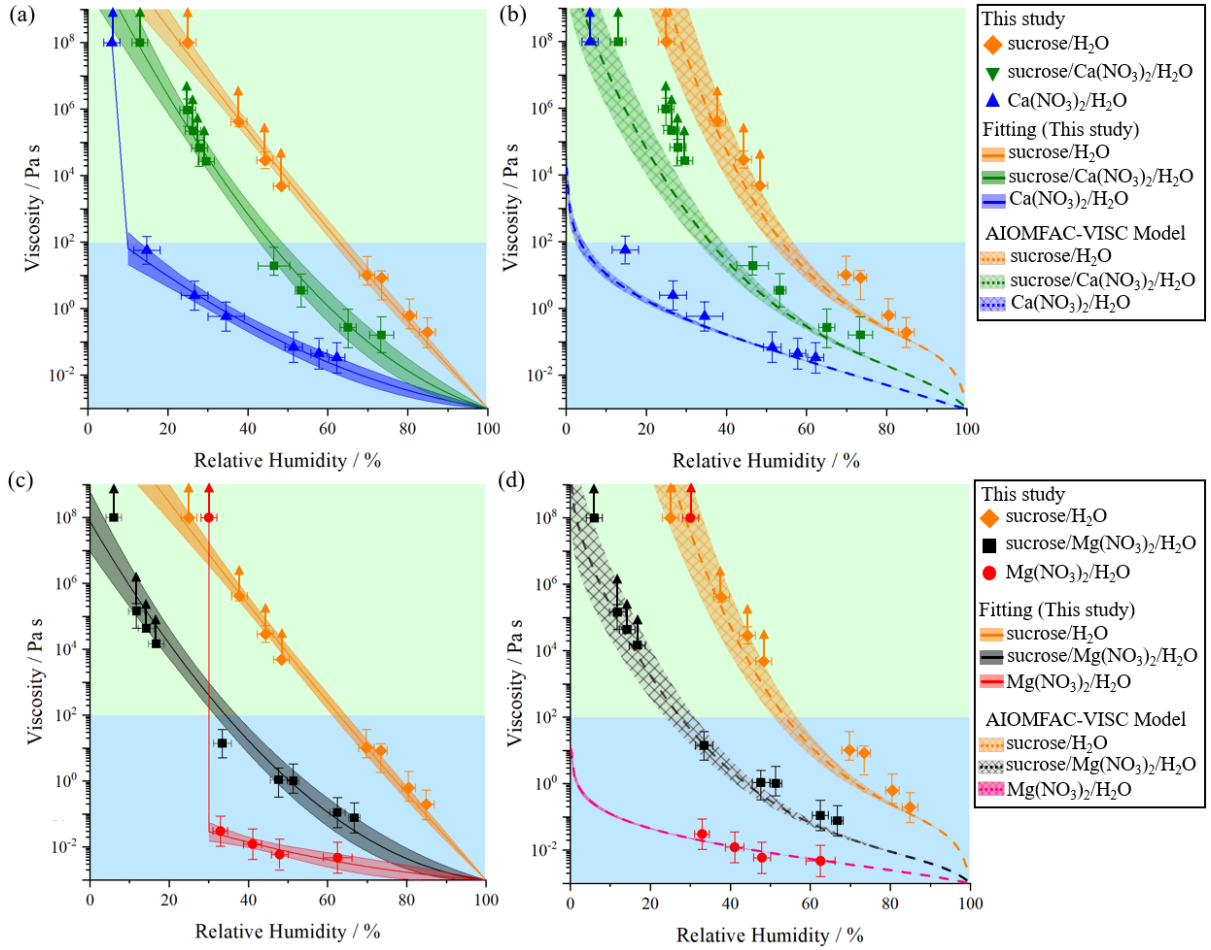

Figure 4. Comparison of viscosities of binary and ternary systems obtained from the bead-mobility and poke-and-flow experiments. (a) Mean viscosities of sucrose/H_2O, $Ca(NO_3)_2/H_2O$, and sucrose/$Ca(NO_3)_2/H_2O$ particles with polynomial fits from measured viscosities for an organic-to-inorganic mass ratio (OIR) of 1:1. All data at a temperature of 293 ± 1 K , (b) Mean viscosities of sucrose/H_2O, $Ca(NO_3)_2/H_2O$ (grouped by relative humidity (RH) using data from Fig. 3), and sucrose/$Ca(NO_3)_2/H_2O$ particles with AIOMFAC-VISC model predictions, (c) mean viscosities of sucrose/H_2O, $Mg(NO_3)_2/H_2O$ (grouped by RH using data from Fig. 3), and sucrose/$Mg(NO_3)_2/H_2O$ particles with polynomial fits from measured viscosities for an OIR of 1:1, (d) mean viscosities of sucrose/H_2O, $Mg(NO_3)_2/H_2O$, and sucrose/$Mg(NO_3)_2/H_2O$ particles with AIOMFAC-VISC model predictions. The error bars in RH were generated from the RH uncertainty and the standard deviation of individual data grouped by RH. The error bars in viscosity represent grouped viscosity by RH including

at least 3 data points. Symbols marked with upward arrows represent lower limits of the viscosities of the particles calculated based on the experimental flow time period and the equation reported in Sellier et al. (2015). Fitting (solid line curves and shaded areas) from measured viscosities are based on 2nd polynomial curve fits with 95% confidence bands. Predictions (dash line curves with checker shaded areas) are based on from AIOMFAC-VISC model. The parameterizations are described in Sect. S3 and Table S1. Light blue and green regions represent liquid and semi-solid phase state ranges, respectively.

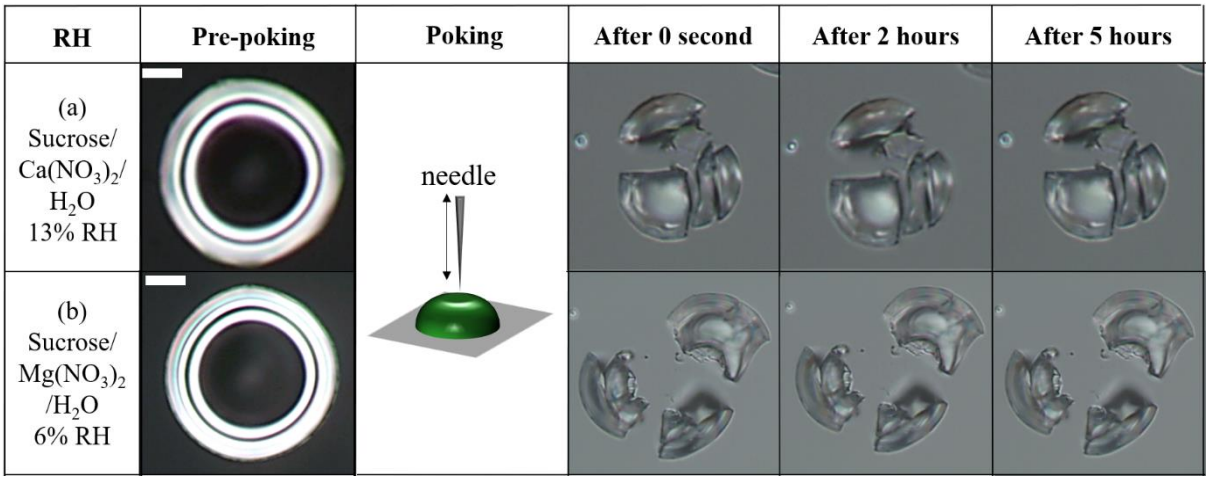

Figure 5. Optical images during poke-and-flow experiments at the points of pre-poking, poking, and post-poking for particles consisting of (a) sucrose/$Ca(NO_3)_2$/H_2O particles and (b) sucrose/$Mg(NO_3)_2$/H_2O particles for relative humidity (RH) where the particles shattered. The scale bar indicates 5 µm.

References

Abdulagatov, I. M., Zeinalova, A. A. and Azizov, N. D.: Viscosity of the aqueous $Ca(NO_3)_2$ solutions at temperatures from 298 to 573 K and at pressures up to 40 MPa, J. Chem. Eng. Data, 49(5), 1444–1450, doi:10.1021/je049853n, 2004.

Athanasiadis, A., Fitzgerald, C., Davidson, N. M., Giorio, C., Botchway, S. W., Ward, A. D., Kalberer, M., Pope, F. D. and Kuimova, M. K.: Dynamic viscosity mapping of the oxidation of squalene aerosol particles, Phys. Chem. Chem. Phys., 18, 30385–30393, doi:10.1039/C6CP05674A, 2016.

Barbaro, E., Kirchgeorg, T., Zangrando, R., Vecchiato, M., Piazza, R., Barbante, C. and Gambaro, A.: Sugars in Antarctic aerosol, Atmos. Environ., 118, 135–144, doi:10.1016/j.atmosenv.2015.07.047, 2015.

Bateman, A. P., Bertram, A. K. and Martin, S. T.: Hygroscopic influence on the semisolid-to-liquid transition of secondary organic materials, J. Phys. Chem. A, 119(19), 4386–4395, doi:10.1021/jp508521c, 2015.

Berkemeier, T.; Steimer, S. S.; Krieger, U. K.; Peter, T.; Pöschl, U.; Ammann, M.; Shiraiwa, M. Ozone uptake on glassy, semi-solid and liquid organic matter and the role of reactive oxygen intermediates in atmospheric aerosol chemistry. Phys. Chem. Chem. Phys. 2016, 18, 12662−12674.

Bhattarai, G., Lee, J. B., Kim, M. H., Ham, S., So, H. S., Oh, S., Sim, H. J., Lee, J. C., Song, M. and Kook, S. H.: Maternal exposure to fine particulate matter during pregnancy induces progressive senescence of hematopoietic stem cells under preferential impairment of the bone marrow microenvironment and aids development of myeloproliferative disease, Leukemia, 9–12, doi:10.1038/s41375-019-0665-8, 2019.

Cheng, Z., Luo, L., Wang, S., Wang, Y., Sharma, S., Shimadera, H., Wang, X., Bressi, M., de Miranda, R. M., Jiang, J., Zhou, W., Fajardo, O., Yan, N. and Hao, J.: Status and characteristics of ambient PM2.5 pollution in global megacities, Environ. Int., 89–90, 212–221, doi:10.1016/j.envint.2016.02.003, 2016.

Fu, P., Kawamura, K., Kobayashi, M. and Simoneit, B. R. T.: Seasonal variations of sugars in atmospheric particulate matter from Gosan, Jeju Island: Significant contributions of airborne pollen and Asian dust in spring, Atmos. Environ., 55, 234–239, doi:10.1016/j.atmosenv.2012.02.061, 2012.

Davies, J. F., and Wilson, K. R.: Nanoscale interfacial gradients formed by the reactive uptake of OH radicals onto viscous aerosol surfaces. Chem. Sci., 6, 7020–7027, https://doi.org/10.1039/C5SC02326B, 2015.

George, I.J., Abbatt, J.P.D.: Heterogeneous oxidation of atmospheric aerosol particles by gas-phase radicals. Nature Chemistry 2:713–722, 2010.

Gervasi, N. R., Topping, D. O. and Zuend, A.: A predictive group-contribution model for the viscosity of aqueous organic aerosol, Atmos. Chem. Phys., 20(5), 2987–3008, doi:10.5194/acp-20-2987-2020, 2020.

Grayson, J. W., Song, M., Sellier, M. and Bertram, A. K.: Validation of the poke-flow technique combined with simulations of fluid flow for determining viscosities in samples with small volumes and high viscosities, Atmos. Meas. Tech., 8(6), 2463–2472, doi:10.5194/amt-8-2463-2015, 2015.

Grayson, J. W., Zhang, Y., Mutzel, A., Renbaum-Wolff, L., Böge, O., Kamal, S., Herrmann, H., Martin, S. T. and Bertram, A. K.: Effect of varying experimental conditions on the viscosity of α-pinene derived secondary organic material, Atmos. Chem. Phys., 16(10), 6027–6040, doi:10.5194/acp-16-6027-2016, 2016a.

Grayson, J. W., Song, M., Evoy, E., Upshur, M. A., Ebrahimi, M., Geiger, F. M., Thomson, R. J. and Bertram, A. K.: The effect of adding hydroxyl functional groups and increasing molar mass on the viscosity of organics relevant to secondary organic aerosols, Atmos. Chem. Phys., 17, 8509–8524, doi:10.5194/acp-2016-672, 2016b.

Gupta, D., Eom, H. J., Cho, H. R., and Ro, C. U.: Gupta, D., Eom, H.-J., Cho, H.-R., and Ro, C.-U.: Hygroscopic behavior of NaCl- $MgCl_2$ mixture particles as nascent sea-spray aerosol surrogates and observation of efflorescence during humidification, Atmos. Chem. Phys., 15, 11273–11290, https://doi.org/10.5194/acp-15- 11273-2015, 2015

Hao, L. Q., Kortelainen, A., Romakkaniemi, S., Portin, H., Jaatinen, A., Leskinen, A., Komppula, M., Miettinen, P., Sueper, D., Pajunoja, A., Smith, J. N., Lehtinen, K. E. J., Worsnop, D. R., Laaksonen, A. and Virtanen, A.: Atmospheric submicron aerosol composition and particulate organic nitrate formation in a boreal forestland-urban mixed region, Atmos. Chem. Phys., 14(24), 13483–13495, doi:10.5194/acp-14-13483-2014, 2014.

Haynes, W. M.: CRC handbook of chemistry and physics, 97rd ed., CRC Press, New York., 2015.

Heald, C. L., Ridley, D. A., Kreidenweis, S. M. and Drury, E. E.: Satellite observations cap the atmospheric organic aerosol budget, Geophys. Res. Lett., 37(24), 1–5, doi:10.1029/2010GL045095, 2010.

Hinks, M. L., Brady, M. V, Lignell, H., Song, M., Grayson, J. W., Bertram, A. K., Lin, P., Laskin, A., Laskin, J. and Nizkorodov, S. A.: Effect of viscosity on photodegradation rates in complex secondary organic aerosol materials, Phys. Chem. Chem. Phys., 18(13), 8785–8793, doi:10.1039/c5cp05226b, 2016.

Hodas, N.; Zuend, A.; Mui, W.; Flagan, R. C.; Seinfeld, J. H.: Influence of particle-phase state on the hygroscopic behavior of mixed organic–inorganic aerosols, Atmos. Chem. Phys. 2015, 15, 5027−5045

Hosny, N. A., Fitzgerald, C., Vysniauskas, A., Athanasiadis, T., Berkemeier, T., Uygur, N., Pöschl, U., Shiraiwa, M., Kalberer, M., Pope, F. D. and Kuimova, M. K.: Direct imaging of changes in aerosol particle viscosity upon hydration and chemical aging, Chem. Sci., 7, 1357–1367, doi:10.1039/C5SC02959G, 2016.

Huang, R. J., Zhang, Y., Bozzetti, C., Ho, K. F., Cao, J. J., Han, Y., Daellenbach, K. R., Slowik, J. G., Platt, S. M., Canonaco, F., Zotter, P., Wolf, R., Pieber, S. M., Bruns, E. A., Crippa, M., Ciarelli, G., Piazzalunga, A., Schwikowski, M., Abbaszade, G., Schnelle-Kreis, J., Zimmermann, R., An, Z., Szidat, S., Baltensperger, U., El Haddad, I. and Prévôt, A. S. H.: High secondary aerosol contribution to particulate pollution during haze events in China, Nature, 514(7521), 218–222, doi:10.1038/nature13774, 2015.

Huang, Y., Mahrt, F., Xu, S., Shiraiwa, M., Zuend, A. and Bertram, A. K.: Coexistence of three liquid phases in individual atmospheric aerosol particles, Proc. Natl. Acad. Sci. U. S. A., 118(16), e2102512118, doi:https://doi.org/10.1073/pnas.2102512118, 2021.

Jimenez, J. L., Canagaratna, M. R., Donahue, N. M., Prevot, a. S. H., Zhang, Q., Kroll, J. H., DeCarlo, P. F., Allan, J. D., Coe, H., Ng, N. L., Aiken, a. C., Docherty, K. S., Ulbrich, I. M., Grieshop, A. P., Robinson, a. L., Duplissy, J., Smith, J. D., Wilson, K. R., Lanz, V. a., Hueglin, C., Sun, Y. L., Tian, J., Laaksonen, A., Raatikainen, T., Rautiainen, J., Vaattovaara, P., Ehn, M., Kulmala, M., Tomlinson, J. M., Collins, D. R., Cubison, M. J., Dunlea, J., Huffman, J. A., Onasch, T. B., Alfarra, M. R., Williams, P. I., Bower, K., Kondo, Y., Schneider, J., Drewnick, F., Borrmann, S., Weimer, S., Demerjian, K., Salcedo, D., Cottrell, L., Griffin, R., Takami, a., Miyoshi, T., Hatakeyama, S., Shimono, A., Sun, J. Y., Zhang, Y. M., Dzepina, K., Kimmel, J. R., Sueper, D., Jayne, J. T., Herndon, S. C., Trimborn, a. M., Williams, L. R., Wood, E. C., Middlebrook, A. M., Kolb, C. E., Baltensperger, U., Worsnop, D. R., Dunlea, E. J., Huffman, J. A., Onasch, T. B., Alfarra, M. R., Williams, P. I., Bower, K., Kondo, Y., Schneider, J.,

Drewnick, F., Borrmann, S., Weimer, S., Demerjian, K., Salcedo, D., Cottrell, L., Griffin, R., Takami, a., Miyoshi, T., Hatakeyama, S., Shimono, A., Sun, J. Y., Zhang, Y. M., Dzepina, K., Kimmel, J. R., Sueper, D., Jayne, J. T., Herndon, S. C., Trimborn, a. M., Williams, L. R., Wood, E. C., Middlebrook, A. M., Kolb, C. E., Baltensperger, U., Worsnop, D. R., Dunlea, J., Huffman, J. A., et al.: Evolution of organic aerosols in the atmosphere, Science (80), 326(5959), 1525–1529, doi:10.1126/science.1180353, 2009.

Steimer, S. S.; Berkemeier, T.; Gilgen, A.; Krieger, K. U.; Peter, T.; Shiraiwa, M.; Ammann, M. Shikimic acid ozonolysis kinetics in the transition from liquid aqueous solution to highly viscous glass. Phys. Chem. Chem. Phys. 2015, 17, 31101–31109. https://doi.org/10.1039/C5CP04544D.

Kanakidou, M., Seinfeld, J. H., Pandis, S. N., Barnes, I., Dentener, F. J., Facchini, M. C., Van Dingenen, R., Ervens, B., Nenes, A., Nielsen, C. J., Swietlicki, E., Putaud, J. P., Balkanski, Y., Fuzzi, S., Horth, J., Moortgat, G. K., Winterhalter, R., Myhre, C. E. L., Tsigaridis, K., Vignati, E., Stephanou, E. G. and Wilson, J.: Organic aerosol and global climate modelling: a review, Atmos. Chem. Phys., 5(4), 1053–1123, doi:10.5194/acp-5-1053-2005, 2005.

Kaufman, Y. J., Tanré, D. and Boucher, O.: A satellite view of aerosols in the climate system, Nature, 419(September), 215–223, 2002.

Kidd, C., Perraud, V., Wingen, L. M. and Finlayson-Pitts, B. J.: Integrating phase and composition of secondary organic aerosol from the ozonolysis of α-pinene., Proc. Natl. Acad. Sci. U. S. A., 111, 7552–7, doi:10.1073/pnas.1322558111, 2014.

Kim, Y., Sartelet, K. and Couvidat, F.: Modeling the effect of non-ideality, dynamic mass transfer and viscosity on SOA formation in a 3-D air quality model, Atmos. Chem. Phys., 19(2), 1241–1261, doi:10.5194/acp-19-1241-2019, 2019.

Knopf, D. A., Alpert, P. and Wang, B.: The role of organic aerosol in atmospheric ice nucleation – A Review, ACS Earth Sp. Chem., acsearthspacechem.7b00120, doi:10.1021/acsearthspacechem.7b00120, 2018.

Koop, T., Bookhold, J., Shiraiwa, M., Pöschl, U. and Poeschl, U.: Glass transition and phase state of organic compounds: dependency on molecular properties and implications for secondary organic aerosols in the atmosphere, Phys. Chem. Chem. Phys., 13(43), 19238–55, doi:10.1039/c1cp22617g, 2011.

Kuwata, M.; Martin, S. T.: Phase of atmospheric secondary organic material affects its reactivity, Proc. Natl. Acad. Sci. U. S. A. 2012, 109, 17354−17359.

Kulmala, M., Asmi, A., Lappalainen, H. K., Baltensperger, U., Brenguier, J. L., Facchini, M. C., Hansson, H. C., Hov, O'Dowd, C. D., Pöschl, U., Wiedensohler, A., Boers, R., Boucher, O., De Leeuw, G., Denier Van Der Gon, H. A. C., Feichter, J., Krejci, R., Laj, P., Lihavainen, H., Lohmann, U., McFiggans, G., Mentel, T., Pilinis, C., Riipinen, I., Schulz, M., Stohl, A., Swietlicki, E., Vignati, E., Alves, C., Amann, M., Ammann, M., Arabas, S., Artaxo, P., Baars, H., Beddows, D. C. S., Bergström, R., Beukes, J. P., Bilde, M., Burkhart, J. F., Canonaco, F., Clegg, S. L., Coe, H., Crumeyrolle, S., D'Anna, B., Decesari, S., Gilardoni, S., Fischer, M., Fjaeraa, A. M., Fountoukis, C., George, C., Gomes, L., Halloran, P., Hamburger, T., Harrison, R. M., Herrmann, H., Hoffmann, T., Hoose, C., Hu, M., Hyvärinen, A., Hõrrak, U., Iinuma, Y., Iversen, T., Josipovic, M., Kanakidou, M., Kiendler-Scharr, A., Kirkevåg, A., Kiss, G., Klimont, Z., Kolmonen, P., Komppula, M., Kristjánsson, J. E., Laakso, L., Laaksonen, A., Labonnote, L., Lanz, V. A., Lehtinen, K. E. J., Rizzo, L. V., Makkonen, R., Manninen, H. E., McMeeking, G., Merikanto, J., Minikin, A., Mirme, S., Morgan, W. T., Nemitz, E., O'Donnell, D., Panwar, T. S., Pawlowska, H., Petzold, A., Pienaar, J. J., Pio, C., Plass-Duelmer, C., Prévôt, A. S. H., Pryor, S., Reddington, C. L., Roberts, G., Rosenfeld, D., Schwarz, J., Seland, O., et al.: General overview: European integrated project on aerosol cloud climate and air quality interactions (EUCAARI)-integrating aerosol research from nano to global scales, Atmos. Chem. Phys., 11(24), 13061–130143, doi:10.5194/acp-11-13061-2011, 2011.

Ladino, L. A., Zhou, S., Yakobi-Hancock, J. D., Aljawhary, D. and Abbatt, J. P. D.: Factors controlling the ice nucleating abilities of α-pinene SOA particles, J. Geophys. Res., 119(14), 9041–9051, doi:10.1002/2014JD021578, 2014.

Laliberté, M. (2007). Model for calculating the viscosity of aqueous aolutions, Journal of Chemical & Engineering Data, 52(4), 1507–1508. https://doi.org/10.1021/je700232s

Laliberté, M. (2009). A model for calculating the heat capacity of aqueous solutions, with updated density and viscosity data. Journal of Chemical & Engineering Data, 54(6), 1725–1760. https://doi.org/10.1021/je8008123

Laskin, A., Iedema, M. J., Ichkovich, A., Graber, E. R., Taraniuk, I. and Rudich, Y.: Direct observation of completely processed calcium carbonate dust particles, Faraday Discuss., 130, 453–468, doi:10.1039/b417366j, 2005.

Li, J., Forrester, S. M., Knopf, D. A.: Heterogeneous oxidation of amorphous organic aerosol surrogates by O3, NO3, and OH at typical tropospheric temperatures. Atmos. Chem. Phys., 20(10), 6055–6080. https://doi.org/10.5194/acp-20-6055-2020, 2020.

Li, X. H., Zhao, L. J., Dong, J. L., Xiao, H. S. and Zhang, Y. H.: Confocal raman studies of $Mg(NO_3)_2$ aerosol particles deposited on a quartz substrate: supersaturated structures and complicated phase transitions, J. Phys. Chem. B, 112(16), 5032–5038, doi:10.1021/jp709938x, 2008.

Lilek, J., and Zuend, A., in preparation, 2020

Liu, Y. J., Zhu, T., Zhao, D. F. and Zhang, Z. F.: Investigation of the hygroscopic properties of Ca(NO3) 2 and internally mixed Ca(NO3)2/CaCO 3 particles by micro-Raman spectrometry, Atmos. Chem. Phys., 8(23), 7205–7215, doi:10.5194/acp-8-7205-2008, 2008.

Mikhailov, E., Vlasenko, S., Martin, S. T., Koop, T. and Pöschl, U.: Amorphous and crystalline aerosol particles interacting with water vapor: conceptual framework and experimental evidence for restructuring, phase transitions and kinetic limitations, Atmos. Chem. Phys., 9(24), 9491–9522, doi:10.5194/acp-9-9491-2009, 2009.

Maclean, A. M., Smith, N. R., Li, Y., Huang, Y., Hettiyadura, A. P. S., Crescenzo, G. V., Shiraiwa, M., Laskin, A., Nizkorodov, S. A. and Bertram, A. K.: Humidity-Dependent Viscosity of Secondary Organic Aerosol from Ozonolysis of β-Caryophyllene: Measurements, Predictions, and Implications, ACS Earth Sp. Chem., 5(2), 305–318, doi:10.1021/acsearthspacechem.0c00296, 2021.

Murphy, D. M., Cziczo, D. J., Froyd, K. D., Hudson, P. K., Matthew, B. M., Middlebrook, A. M., Peltier, R. E., Sullivan, A., Thomson, D. S. and Weber, R. J.: Single-peptide mass spectrometry of tropospheric aerosol particles, J. Geophys. Res. Atmos., 111(23), 1–15, doi:10.1029/2006JD007340, 2006.

Murray, B. J., Wilson, T. W., Dobbie, S., Cui, Z., Al-Jumur, S. M. R. K., Möhler, O., Schnaiter, M., Wagner, R., Benz, S., Niemand, M., Saathoff, H., Ebert, V., Wagner, S. and Kärcher, B.: Heterogeneous nucleation of ice particles on glassy aerosols under cirrus conditions, Nat. Geosci., 3, 233–237, doi:10.1038/ngeo817, 2010.

Pan, X., Uno, I., Wang, Z., Nishizawa, T., Sugimoto, N., Yamamoto, S., Kobayashi, H., Sun, Y., Fu, P., Tang, X. and Wang, Z.: Real-time observational evidence of changing Asian dust morphology with the mixing of heavy anthropogenic pollution, Sci. Rep., 7(1), 1–8, doi:10.1038/s41598-017-00444-w, 2017.

Petters, S. S., Kreidenweis, S. M., Grieshop, A. P., Ziemann, P. J. and Petters, M. D.: Temperature- and humidity-dependent phase states of secondary organic aerosols, Geophys. Res. Lett., 46(2), 1005–1013, doi:10.1029/2018GL080563, 2019.

Power, R. M., Simpson, S. H., Reid, J. P. and Hudson, A. J.: The Transition from liquid to solid-like behaviour in ultrahigh viscosity aerosol particles, Chem. Sci., 4(6), 2597–2604, doi:10.1039/c3sc50682g, 2013.

Reid, J. P., Bertram, A. K., Topping, D. O., Laskin, A., Martin, S. T., Petters, M. D., Pope, F. D. and Rovelli, G.: The viscosity of atmospherically relevant organic particles, Nat. Commun., 9(1), 956, doi:10.1038/s41467-018-03027-z, 2018.

Renbaum-Wolff, L., Grayson, J. W., Bateman, A. P., Kuwata, M., Sellier, M., Murray, B. J., Shilling, J. E., Martin, S. T. and Bertram, A. K.: Viscosity of α-pinene secondary organic material and implications for particle growth and reactivity., Proc. Natl. Acad. Sci. U. S. A., 110(20), 8014–9, doi:10.1073/pnas.1219548110, 2013.

Richards, D. S., Trobaugh, K. L., Hajek-Herrera, J., Price, C. L., Sheldon, C. S., Davies, J. F., Davis, R. D.: Ion-molecule interactions enable unexpected phase transitions in organic-inorganic aerosol. Sci. Adv., 6 (47), 1–12. https://doi.org/10.1126/sciadv.abb5643, 2020a.

Richards, D. S., Trobaugh, K. L., Hajek-Herrera, J. and Davis, R. D.: Dual-Balance Electrodynamic Trap as a Microanalytical Tool for Identifying Gel Transitions and Viscous Properties of Levitated Aerosol Particles, Anal. Chem., 92(4), 3086–3094, doi:10.1021/acs.analchem.9b04487, 2020b

Rothfuss, N. E. and Petters, M. D.: Influence of functional groups on the viscosity of organic aerosol, Environ. Sci. Technol., 51, 271–279, doi:10.1021/acs.est.6b04478, 2017.

Rovelli, G., Song, Y. C., Maclean, A. M., Topping, D. O., Bertram, A. K. and Reid, J. P.: Comparison of approaches for measuring and predicting the viscosity of ternary component aerosol particles, Anal. Chem., 91, 5074−5082, doi:10.1021/acs.analchem.8b05353, 2019.

Russell, P. B., Kinne, S. A. and Bergstrom, R. W.: Aerosol climate effects: local radiative forcing and column closure experiments, J. Geophys. Res. Atmos., 102(D8), 9397–9407, doi:10.1029/97jd00112, 1997.

Saukko, E., Lambe, A. T., Massoli, P., Koop, T., Wright, J. P., Croasdale, D. R., Pedernera, D. A., Onasch, T. B., Laaksonen, A., Davidovits, P., Worsnop, D. R. and Virtanen, A.: Humidity-dependent phase state of SOA particles from biogenic and anthropogenic precursors, Atmos. Chem. Phys., 12(16), 7517–7529, doi:10.5194/acp-12-7517-2012, 2012.

Schill, G. P., De Haan, D. O. and Tolbert, M. a.: Heterogeneous ice nucleation on simulated secondary organic aerosol, Environ. Sci. Technol., 48(3), 1675–1682, doi:10.1021/es4046428, 2014.

Schmedding, R., Rasool, Q. Z., Zhang, Y., Pye, H. O. T., Zhang, H., Chen, Y., Surratt, J. D., Lopez-Hilfiker, F. D., Thornton, J. A., Goldstein, A. H. and Vizuete, W.: Predicting secondary organic aerosol phase state and viscosity and its effect on multiphase chemistry in a regional-scale air quality model, Atmos. Chem. Phys., 20(13), 8201–8225, doi:10.5194/acp-20-8201-2020, 2020.

Shi, Z., Zhang, D., Hayashi, M., Ogata, H., Ji, H. and Fujiie, W.: Influences of sulfate and nitrate on the hygroscopic behaviour of coarse dust particles, Atmos. Environ., 42(4), 822–827, doi:10.1016/j.atmosenv.2007.10.037, 2008.

Shiraiwa, M. and Seinfeld, J. H.: Equilibration timescale of atmospheric secondary organic aerosol partitioning, Geophys. Res. Lett., 39, L24801, doi:10.1029/2012GL054008, 2012.

Slade, J. H., and Knopf, D. A.: Multiphase OH oxidation kinetics of organic aerosol: The role of particle phase state and relative humidity. Geophys. Res. Lett., 41(14), 5297–5306. https://doi.org/10.1002/2014GL060582, 2014.

Song, M., Liu, P. F., Hanna, S. J., Li, Y. J., Martin, S. T. and Bertram, a. K.: Relative humidity-dependent viscosities of isoprene-derived secondary organic material and atmospheric implications for isoprene-dominant forests, Atmos. Chem. Phys., 15, 5145–5159, doi:10.5194/acp-15-5145-2015, 2015.

Song, M., Liu, P. F., Hanna, S. J., Zaveri, R. A., Potter, K., You, Y., Martin, S. T. and Bertram, A. K.: Relative humidity-dependent viscosity of secondary organic material from toluene photo-oxidation and possible implications for organic particulate matter over megacities, Atmos. Chem. Phys., 16(14), 8817–8830, doi:10.5194/acp-16-8817-2016, 2016a.

Song, M., Maclean, A. M., Huang, Y., Smith, N. R., Blair, S. L., Laskin, J., Laskin, A., DeRieux, W.-S. W., Li, Y., Shiraiwa, M., Nizkorodov, S. A. and Bertram, A. K.: Liquid-liquid phase separation and viscosity within secondary organic aerosol generated from diesel fuel vapors, Atmos. Chem. Phys., 19(19), 12515–12529, doi:10.5194/acp-2019-367, 2019.

Song, Y. C., Ryu, J., Malek, M. A., Jung, H. J. and Ro, C. U.: Chemical speciation of individual airborne particles by the combined use of quantitative energy-dispersive electron probe X-ray microanalysis and attenuated total reflection Fourier transform-infrared imaging techniques, Anal. Chem., 82(19), 7987–7998, doi:10.1021/ac1014113, 2010.

Song, Y. C., Eom, H. J., Jung, H. J., Malek, M. A., Kim, H. K., Geng, H. and Ro, C. U.: Investigation of aged Asian dust particles by the combined use of quantitative ED-EPMA and ATR-FTIR imaging, Atmos. Chem. Phys., 13(6), 3463–3480, doi:10.5194/acp-13-3463-2013, 2013.

Song, Y. C., Haddrell, A. E., Bzdek, B. R., Reid, J. P., Bannan, T., Topping, D. O., Percival, C. and Cai, C.: Measurements and pedictions of binary component aerosol particle viscosity, J. Phys. Chem. A, 120(41), 8123–8137, doi:10.1021/acs.jpca.6b07835, 2016b.

Stokes, R. H., & Robinson, R. A. (1966). Interactions in aqueous nonelectrolyte solutions .i. solute-solvent equilibria. *J. Phys. Chem.*, *70*(7), 2126–2130.

Sullivan, R. C., Guazzotti, S. A., Sodeman, D. A. and Prather, K. A.: Direct observations of the atmospheric processing of Asian mineral dust, Atmos. Chem. Phys., 7(5), 1213–1236, doi:10.5194/acp-7-1213-2007, 2007.

Shiraiwa, M.; Ammann, M.; Koop, T.; Poschl, U.: Gas uptake and chemical aging of semisolid organic aerosol particles, Proc. Natl. Acad. Sci. U. S. A. 2011, 108, 11003−11008.

Usher, C. R., Michel, A. E. and Grassian, V. H.: Reactions on mineral dust, Chem. Rev., 103(12), 4883–4939, doi:10.1021/cr020657y, 2003.

Vaden, T. D., Imre, D., Beranek, J., Shrivastava, M. and Zelenyuk, A.: Evaporation kinetics and phase of laboratory and ambient secondary organic aerosol, Proc. Natl. Acad. Sci. U. S. A., 108(6), 2190–2195, doi:10.1073/pnas.1013391108, 2011.

Virtanen, A., Joutsensaari, J., Koop, T., Kannosto, J., Yli-Pirilä, P., Leskinen, J., Mäkelä, J. M., Holopainen, J. K., Pöschl, U., Kulmala, M., Worsnop, D. R. and Laaksonen, A.: An amorphous solid state of biogenic secondary organic aerosol particles., Nature, 467, 824–7, doi:10.1038/nature09455, 2010.

Wahab, A., Mahiuddin, S., Hefter, G. and Kunz, W.: Densities, ultrasonic velocities, viscosities, and electrical conductivities of aqueous solutions of $Mg(OAc)_2$ and $Mg(NO_3)_2$, J. Chem. Eng. Data, 51(5), 1609–1616, doi:10.1021/je060107n, 2006.

Wallace, B. J. and Preston, T. C.: Water Uptake and Loss in Viscous Aerosol Particles with Concentration-Dependent Diffusivities, J. Phys. Chem. A, 123(15), 3374–3382, doi:10.1021/acs.jpca.9b00907, 2019.

Wang, B., Lambe, A. T., Massoli, P., Onasch, T. B., Davidovits, P., Worsnop, D. R. and Knopf, D. A.: The deposition ice nucleation and immersion freezing potential of amorphous secondary organic aerosol: Pathways for ice and mixed-phase cloud formation, J. Geophys. Res., 117(16), 1–12, doi:10.1029/2012JD018063, 2012.

Wang, G., Zhang, R., Gomez, M. E., Yang, L., Levy Zamora, M., Hu, M., Lin, Y., Peng, J., Guo, S., Meng, J., Li, J., Cheng, C., Hu, T., Ren, Y., Wang, Y., Gao, J., Cao, J., An, Z., Zhou, W., Li, G., Wang, J., Tian, P., Marrero-Ortiz, W., Secrest, J., Du, Z., Zheng, J., Shang, D., Zeng, L., Shao, M., Wang, W., Huang, Y., Wang, Y., Zhu, Y., Li, Y., Hu, J., Pan, B., Cai, L., Cheng, Y., Ji, Y., Zhang, F., Rosenfeld, D., Liss, P. S., Duce, R. A., Kolb, C. E. and Molina, M. J.: Persistent sulfate formation from London fog to Chinese haze, Proc. Natl. Acad. Sci., 113(48), 13630–13635, doi:10.1073/pnas.1616540113, 2016.

Wang, S., Nan, J., Shi, C., Fu, Q., Gao, S., Wang, D., Cui, H., Saiz-Lopez, A. and Zhou, B.: Atmospheric ammonia and its impacts on regional air quality over the megacity of Shanghai, China, Sci. Rep., 5(May), 1–13, doi:10.1038/srep15842, 2015a.

Wang, Y., Ma, J. B., Zhou, Q., Pang, S. F. and Zhang, Y. H.: Hygroscopicity of mixed glycerol/$Mg(NO_3)_2$/water droplets affected by the interaction between magnesium ions and glycerol molecules, J. Phys. Chem. B, 119(17), 5558–5566, doi:10.1021/acs.jpcb.5b00458, 2015b.

Wilson, T. W., Murray, B. J., Wagner, R., Möhler, O., Saathoff, H., Schnaiter, M., Skrotzki, J., Price, H. C., Malkin, T. L., Dobbie, S. and Al-Jumur, S. M. R. K.: Glassy aerosols with a range of compositions

nucleate ice heterogeneously at cirrus temperatures, Atmos. Chem. Phys., 12(18), 8611–8632, doi:10.5194/acp-12-8611-2012, 2012.

Winston, P. W. and Bates, D. H.: Saturated solutions for the control of humidity in biological research, Ecology, 41(1), 232–237, 1960.

Yli-Juuti, T., Pajunoja, A., Tikkanen, O. P., Buchholz, A., Faiola, C., Väisänen, O., Hao, L., Kari, E., Peräkylä, O., Garmash, O., Shiraiwa, M., Ehn, M., Lehtinen, K. and Virtanen, A.: Factors controlling the evaporation of secondary organic aerosol from α-pinene ozonolysis, Geophys. Res. Lett., 44(5), 2562–2570, doi:10.1002/2016GL072364, 2017.

Zdanovskii, A. B. (1936). Trudy Solyanoi Laboratorii (Transactions of the Salt Laboratory), *Akad. Nauk SSSR, 6*, 5–70.

Zdanovskii, A. B. (1948). New methods of calculating solubilities of electrolytes in multicomponent systems. *Zh. Fiz. Khim.*, *22*(12), 1478–1485.

Zhang, Q., Jimenez, J. L., Canagaratna, M. R., Allan, J. D., Coe, H., Ulbrich, I., Alfarra, M. R., Takami, A., Middlebrook, A. M., Sun, Y. L., Dzepina, K., Dunlea, E., Docherty, K., DeCarlo, P. F., Salcedo, D., Onasch, T., Jayne, J. T., Miyoshi, T., Shimono, A., Hatakeyama, S., Takegawa, N., Kondo, Y., Schneider, J., Drewnick, F., Borrmann, S., Weimer, S., Demerjian, K., Williams, P., Bower, K., Bahreini, R., Cottrell, L., Griffin, R. J., Rautiainen, J., Sun, J. Y., Zhang, Y. M. and Worsnop, D. R.: Ubiquity and dominance of oxygenated species in organic aerosols in anthropogenically-influenced Northern Hemisphere midlatitudes, Geophys. Res. Lett., 34(13), 1–6, doi:10.1029/2007GL029979, 2007.

Zhang, R., Wang, G., Guo, S., Zamora, M. L., Ying, Q., Lin, Y., Wang, W., Hu, M. and Wang, Y.: Formation of urban fine particulate matter, Chem. Rev., 115(10), 3803–3855, doi:10.1021/acs.chemrev.5b00067, 2015a.

Zhang, Y., Sanchez, M. S., Douet, C., Wang, Y., Bateman, A. P., Gong, Z., Kuwata, M., Renbaum-Wolff, L., Sato, B. B., Liu, P. F., Bertram, A. K., Geiger, F. M. and Martin, S. T.: Changing shapes and implied viscosities of suspended submicron particles, Atmos. Chem. Phys., 15(14), 7819–7829, doi:10.5194/acp-15-7819-2015, 2015b.

Zieger, P., Vaisanen, O., Corbin, J. C., Partridge, D. G., Bastelberger, S., Mousavi-Fard, M., Rosati, B., Gysel, M., Krieger, U. K., Leck, C., Nenes, A., Riipinen, I., Virtanen, A., and Salter, M. E.: Revising the

hygroscopicity of inorganic sea salt particles, Nat. Commun., 8, 15883, https://doi.org/10.11038/ncomms15883, 2017.

Zobrist, B., Marcolli, C., Pedernera, D. A. and Koop, T.: Do atmospheric aerosols form glasses?, Atmos. Chem. Phys., 8(3), 5221–5244, 2008.

Zobrist, B., Soonsin, V., Luo, B. P., Krieger, U. K., Marcolli, C., Peter, T. and Koop, T.: Ultra-slow water diffusion in aqueous sucrose glasses., Phys. Chem. Chem. Phys., 13(8), 3514–26, doi:10.1039/c0cp01273d, 2011.

Zuend, A., Marcolli, C., Booth, A. M., Lienhard, D. M., Soonsin, V., Krieger, U. K., Topping, D. O., McFiggans, G., Peter, T., & Seinfeld, J. H., New and extended parameterization of the thermodynamic model AIOMFAC: Calculation of activity coefficients for organic-inorganic mixtures containing carboxyl, hydroxyl, carbonyl, ether, ester, alkenyl, alkyl, and aromatic functional groups., Atmos. Chem. Phys., 11(17), 9155–9206. https://doi.org/10.5194/acp-11-9155-2011, 2011

Zuend, A., Marcolli, C., Luo, B. P., & Peter, T., A thermodynamic model of mixed organic-inorganic aerosols to predict activity coefficients. Atmos. Chem. Phys., 35, 2008.

Xiao, S., Bertram, A.K.: Reactive uptake kinetics of NO3 on multicomponent and multiphase organic mixtures containing unsaturated and saturated organics. Phys. Chem. Chem. Phys.13:6628–6636, 2011.

Xu, R.; Ki Lam, H.; R Wilson, K.; F Davies, J.; Song, M.; Li, W.; Tse, Y. L. S.; Nin Chan, M. Effect of inorganic-to-organic mass ratio on the heterogeneous OH reaction rates of erythritol: implications for atmospheric chemical stability of 2-mthyltetrols. Atmos. Chem. Phys., 20 (6), 3879–3893. https://doi.org/10.5194/acp-20-3879-2020, 2020